

Interaction patterns and diversity in assembled ecological communities

Guy Bunin

Department of Physics, Massachusetts Institute of Technology, Cambridge, Massachusetts 02139, USA

The assembly of ecological communities from a pool of species is central to ecology, but the effect of this process on properties of community interaction networks is still largely unknown. Here, we use a systematic analytical framework to describe how assembly from a species pool gives rise to community network properties that differ from those of the pool: Compared to the pool, the community shows a bias towards higher carrying capacities, weaker competitive interactions and stronger beneficial interactions. Moreover, even if interactions between all pool species are completely random, community networks are more structured, with correlations between interspecies interactions, and between interactions and carrying capacities. Nonetheless, we show that these properties are not sufficient to explain the coexistence of all community species, and that it is a simple relation between interactions and species abundances that is responsible for the diversity within a community.

Networks of species interactions and their structure are central objects of study in community ecology, both in terms of the organization of the links and the strength of the interactions. Network structure has been related to increase in maximal diversity and species abundance [1, 11] and to ecosystem functioning [2, 3]. Interaction patterns tell us about underlying mechanisms of interaction such as competition over resources, and about the evolutionary and assembly history of the community [4]. In addition, the network structure is shaped by the requirements of stability [5–7] both internally and in the face of migration to and from a pool of available species [8, 9]. The resulting abundances must be positive, a requirement known as feasibility [10–12]. Such constraints are especially important in conditions where interactions are a dominant factor [9, 13].

These constraints imply that viable communities are not arbitrary collections of species from the pool, but instead have special properties. This is expected to affect the network properties. For example, species that suffer from strong competition are less likely to persist, so weaker competitive interactions might be over-represented in the community, as was indeed observed in simulations [14]. Similarly, species with higher carrying capacities might have better chances to persist, biasing this distribution with respect to that of the entire pool. Beyond such considerations, a framework giving definite, quantitative predictions for these effects, and for the emergence of more complex patterns has thus far been lacking.

To shed light on this process we turn to community assembly models, where the interactions between all species in the pool – as would be measured in the local conditions – are modeled. Such models have provided insight into the influence of the assembly process and the existence of multiple equilibria [15–25], the resulting species abundance [26–28, 30], growth of resistance to invasion [19, 21, 22], the effects of noise and rates of relaxation following a change in the community [13, 24–27], and ecosystem function [31]. Works within this framework have recognized that the properties of the community network are different from those of the entire pool. In

simulations, the mean interaction strengths were found to be smaller in the community [14]; and certain combinations of productivities and interspecies interactions were found appear more commonly than others [29, 30]. No systematic account of such differences has been provided.

In this work we study how network properties are influenced by the constraints of community assembly from a given species pool, through a systematic framework giving analytical predictions. Our aim is two fold. First, to describe how the statistical properties of the network are altered when restricted to interactions inside viable communities, see Fig. 1(a,b). Even if interactions between all pool species are “maximally random”, comprised of a single trophic level with random uncorrelated interactions between species, the community networks are found to be structured. This is significant in light of the large body of work, following [32], that models communities using random interactions. The changes in statistical properties include correlations between interspecies interactions, and between them and the carrying capacities. In addition, carrying capacities are on average higher than in the pool, and interspecies interactions are less competitive or more beneficial.

Secondly, focusing on the assembled community we ask: how does its network allow all community species to coexist? After all, the persistence of the community species is somehow encoded in the network structure. It turns out that correlations between interactions play a crucial role in allowing for higher diversity. But finally, it is a simple relation between interspecies interactions and species abundances that fully accounts for the coexistence of all species in the community.

The model includes a pool of species, a subset of which forms the community, whose members are the persistent species (those whose abundance does not decay to zero). The community must be resistant to invasion by pool species outside it, so that an invader’s abundance decays if it is introduced in small abundance. This criterion accounts for the effect of migration, if migration acts on long enough time-scales which allow the community to relax between colonization attempts [11, 17, 19, 20, 25].

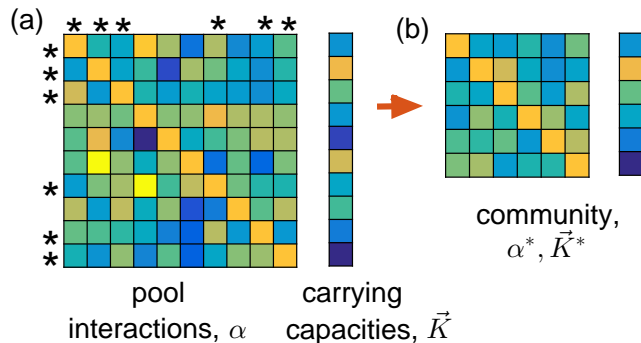


Figure 1. The assembly process generates community networks with properties different from in the pool. (a) The strength of interspecies interactions between all species in the pool, and their carrying capacities. A subset of species (marked by stars) forms the local community. (b) The reduced matrix of community interspecies interactions, and the reduced vector of carrying capacities. They have new statistical properties, including changes in the elements' distributions, correlations between interactions, and between interactions and carrying capacities.

The dynamics of the abundances N_i of the S species in the pool, with $i = 1..S$, are modeled by the generalized Lotka-Volterra equation

$$\frac{dN_i}{dt} = \frac{r_i}{K_i} N_i \left(K_i - N_i - \sum_{j, (j \neq i)} \alpha_{ij} N_j \right). \quad (1)$$

r_i are the intrinsic growth-rates, K_i are the carrying capacities, and α_{ij} for $i \neq j$ encode interspecies interactions with positive values representing competition. The analytical techniques can be applied to a broad class of other models.

In order to proceed, the parameters r_i, K_i and α_{ij} of the species in the pool – as would be measured in the local conditions – need to be specified. Assuming that detailed information on all these parameters is not available, we turn to a null model in which they are sampled at random. Ever since the pioneering work of May [32], models with random parameters have played an important role in theoretical ecology. However, in contrast to Ref. [32], here the community interactions are not drawn at random, and characterizing their emergent structure is the aim of this work. Using a simple null model for the pool allows to disentangle the effects of the assembly process from other factors influencing interaction patterns, for example the mechanisms that generate the interactions such as competition of resources.

The interspecies interactions are thus sampled independently except for possibly a correlation between α_{ij} and α_{ji} , set by the coefficient $\gamma \equiv \text{corr}(\alpha_{ij}, \alpha_{ji})$, so that $-1 \leq \gamma \leq 1$. It is not restricted to the symmetric case, $\gamma = 1$. α_{ij} can have any distribution, as long as it is not long-tailed (see Appendix A for the technical condition). Carrying capacities may vary between species,

in which case they are sampled independently. Results are presented for a normal distribution of K_i for which the analytical expressions are compact; The main conclusions remain unchanged for other distributions. By rescaling $N_i \rightarrow N_i / \text{mean}(K_i)$ we set $\text{mean}(K_i) = 1$.

The analytical framework follows a long tradition in ecology, of adding a species and asking whether it can invade [33], but goes beyond this to analyze the probability for it to invade and its abundance if it succeeded. This is known as the cavity method in the physics literature [16, 26, 27, 34, 35], which in ecological contexts has been used to calculate species abundance distributions and other quantities, such as whether multiple equilibria exist [16, 23, 26–28, 30]. Here, in order to study the community network, we note that its properties can be obtained by conditioning on the persistence of the species involved. For example, the probability distribution of a community interaction strength α_{ij}^* is by definition given by $\text{Pr}(\alpha_{ij}^*) = \text{Pr}(\alpha_{ij} | N_i > 0, N_j > 0)$, where N_i, N_j are the abundances after a long time. This quantity is calculated by introducing two species and asking that they both persist. Joint distributions of multiple interactions and carrying capacities are similarly obtained by conditioning on the persistence of all the species involved. This provides systematic access to all moments and marginal probability distributions of the community network.

The analytical technique is controlled at large pool sizes S with individually weak interspecies interactions, i.e. keeping the asymmetry γ and the parameters $\mu \equiv S \text{mean}(\alpha_{ij})$ and $\sigma^2 \equiv S \text{var}(\alpha_{ij})$ constant. Good agreement with numerical simulations is found for modest number of species, see Fig. 3,4 for $S = 15$ and communities down to 6-7 species. Qualitative agreement – in particular, the sign of correlations – is found for all systems sizes, both for Gaussian and uniform distributions of α_{ij} , see Appendix C. This encompasses systems with purely competitive interactions (α_{ij} are all positive), as well as ones that include mixtures of competitive and beneficial interactions.

I. RESULTS

The results section is organized as follows. First, properties of the interspecies interactions and carrying capacities are presented. Then the relation between network properties and species coexistence is addressed. The results are compared with numerical simulations, described in Appendix D. Derivations are given in Appendix A. Analytical expressions are quoted to lowest order in $1/S$.

Before turning to the community network, we briefly describe the dynamical behavior of the model. It exhibits three distinct regimes, or ‘phases’, depending on the model parameters (μ, σ, γ and the distribution of K_i), separated by sharp boundaries when S is large at fixed μ, σ , see Fig. 2. Details are given in Appendix B. The analytical results are exact in the unique equilibrium phase, and qualitatively correct in the multiple attractors phase,

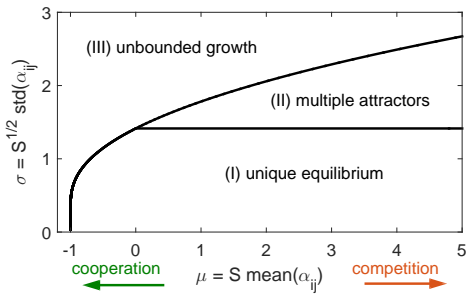


Figure 2. The model exhibits three distinct dynamical behaviors, depending on model parameters. In phase I, a unique stable equilibrium that is resistant to invasion exists for any system. In phase II, multiple dynamical attractors exist, which may be stable equilibria or other attractors such as limit cycles, and the community composition depends assembly history. In phase III, abundances grow without bound; Here the Lotka-Volterra equations likely break down and this phase will not be discussed. The phases are shown for asymmetric interactions ($\gamma = 0$) and equal carrying capacities, all set to $K_i = 1$.

as seen by comparing with numerics. In a third phase the abundances grow without bound; here the description in terms of Lotka-Volterra equations probably breaks down and this regime will not be further discussed.

A. properties of the community network

This section describes properties of community networks. Throughout, α^* , \vec{K}^* and \vec{N}^* will denote the network parameters and abundances restricted to the community species, and S^* the number of species in the community. The pair α^*, \vec{K}^* , will have different properties from α, \vec{K} of the pool. We begin with properties of α^* . The distribution of an element α_{ij}^* is a function both of its distribution over all interactions between species in the pool, and of the assembly process. The assembly enhances the distribution at more negative values, corresponding to weaker competition or stronger beneficial interactions. This enhancement is linear in interaction, $\Pr(\alpha_{ij}^* = \alpha) / \Pr(\alpha_{ij} = \alpha) = 1 - c \cdot \alpha$, see Fig. 3(a,b). The prefactor c depends on the model parameters, and is given in Appendix A. This change shifts the overall mean, $\langle \alpha_{ij}^* \rangle$, towards lower competition than in the pool, Fig. 3(b,c). A drop in the mean competition has been described [14], using simulations. The enhancement of weak competitive links is in line with arguments for the prevalence and importance of weak links [7, 14, 36, 37]. Note however that beneficial interactions, if they exist in the pool, would be more enhanced when their strength $|\alpha_{ij}^*|$ is larger.

In Fig. 3, as everywhere else, simulation data fits perfectly for large S in the unique equilibrium phase.

Pairs of community interaction elements $\alpha_{ij}^*, \alpha_{kl}^*$ that share a species (i.e. belong to the same row or column

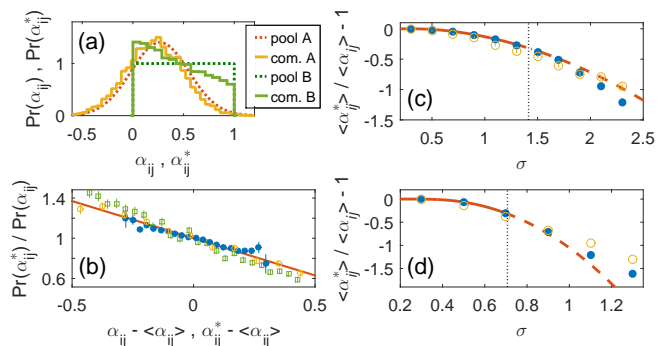


Figure 3. Changes to interspecies interactions. (a) The distribution of interspecies interactions (solid lines) is enhanced at lower values – less competitive or more beneficial – as compared to the pool (dotted lines). (b) The enhancement factor is a linear function of the interaction strength. (c,d) This shifts the mean of α_{ij} , reducing mean competition, shown for $\gamma = 0$ (c) and $\gamma = 1$ (d). In (b,c,d), solid and dashed lines are analytical predictions, which fit perfectly to numerics at large S (full circles) in the unique equilibrium phase (left of vertical dotted line in (c,d)). Open circles are numerical results for Gaussian distribution of α_{ij} and $S = 15$, generating communities with down to around 6 species. Diamonds in (b) are uniform distribution of α_{ij} on $[0, 1]$, and $S = 15$. Gaussian distributions run with $\mu = 4$. In (b) all models have $\sigma = \sqrt{5}/2$, as for the model with α_{ij} uniform on $[0, 1]$.

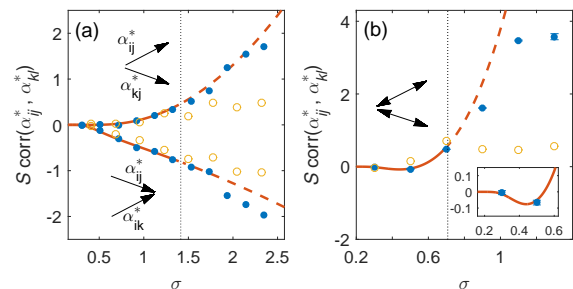


Figure 4. Correlations between interactions that share a species, for (a) asymmetric interactions, $\gamma = 0$ and (b) symmetric interactions, $\gamma = 1$. In (b) there is only one correlation between adjacent interactions, since the interactions are symmetric. Inset shows a part of the same graph, where the correlation changes sign. These correlations are zero when taken over the entire species pool, demonstrating that the community network has new structure not found in the pool. Solid and dashed lines indicate analytical predictions. Simulations at large S (full circles) agree perfectly with theory in phase one. Open circles are numerical results for $S = 15$. Here $\mu = 4$.

of the matrix) are correlated, see Fig. 4. The sign of the correlation may depend on the role of the species in common. For example, in asymmetric systems ($\gamma = 0$), one finds a positive correlation between α_{ij}^* and α_{kj}^* , which corresponds the influence of one species (j) on two others, but negative correlations in the opposite scenario where

two species influence the same species. (Species j influences i with strength α_{ij} through the term $-\alpha_{ij}N_j$ in Eq. (1) for dN_i/dt .) Symmetric interactions ($\gamma = 1$) have only one distinct type of correlation, which changes sign as a function of model parameters, see Fig. 4(b). Correlations between interaction strengths that do not share a common species are weaker (higher order in $1/S$) and are not discussed here. All these quantities are zero when measured over α of the entire species pool, demonstrating that the community interactions indeed have different statistical properties from the pool interactions, or from any model in which interaction strengths are sampled independently.

Moving on to the carrying capacities, when the carrying capacity K_i varies from one species to another, its distribution in the community is altered as compared to that in the pool. This is because species with higher carrying capacities are more likely to be included in the community, see Fig. 5(a). In the limiting case of identical interspecies interactions, the persistent species are simply those whose carrying capacity lies above some threshold. In the other extreme, of large variability of interactions strengths (high σ), the carrying capacities have a negligible effect on which species persist, and so their variance is unchanged. This ‘filtering’ increases the mean of the carrying capacities with respect to the pool, see Fig. 5(b). The variance of the distribution may change in either direction. For a Gaussian distribution it is always reduced, see Fig. 5(b); This is expected to happen in similarly-shaped distributions. In other cases the variance may increase, see Appendix A for an example. Smaller variance allows for greater maximal species diversity [11]; It is interesting that the community assembly can act to either reduce or increase the variance. Correlations between interspecies interactions and carrying capacities emerge in the community. Their sign depends on the model parameters and whether the carrying capacity of the influencing or influenced species is included, see Fig. 5(c), (and also Fig. 12 in Appendix A for $\gamma = 1$).

When different species have different carrying capacities, properties of that distribution are altered by the community assembly process. Feasibility restricts the possible combinations of α^* and \vec{K}^* , since in equilibrium $\alpha^* \vec{N}^* = \vec{K}^*$ (with $\alpha_{ii}^* = 1$) and community abundances must be positive. This set of conditions is at the basis of many theoretical arguments [1, 11, 12]. However, for many purposes it is desirable to have more detailed relations between α^* and \vec{K}^* than this set of inequalities. The community assembly model used here has the advantage of producing explicit predictions for the distribution of carrying capacities and its correlations with elements of α^* , as shown in Fig. 5.

B. Network structure and species coexistence

So far, the differences between assembled networks and those formed by arbitrary collections of species were de-

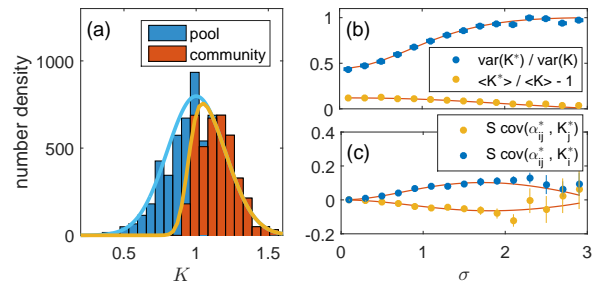


Figure 5. Change in properties of the carrying capacities. (a) Histogram of carrying capacities in the pool and community of a single system, compared to analytical predictions. Higher carrying capacities are more likely to be included in the community. (b) The community has higher mean and smaller variance of carrying capacities than the species pool. (c) Correlations with interspecies interactions emerge, which may be positive or negative. Solid lines are analytical predictions. Model parameters used: $\gamma = 0$, $\sigma_k = 0.2$, and in panel (a), $\sigma = 0.3$.

scribed. By definition, all of the community species coexist in the community. We now ask what properties of the assembled networks, specifically the interspecies interactions, are responsible for this coexistence. To simplify the presentation we focus on communities with identical carrying capacities ($K_i = 1$), so that the community network is specified by the interactions α^* . To better understand the effect of network properties on diversity (number of persistent species), we generate matrices that are the same size as α^* but with different properties. If α^* is replaced by completely random interactions sampled as in the pool, only a fraction of the species persist, see Fig. 6(a,b). Modifying the distribution of individual interactions to match that of the assembled community does little if anything to increase diversity. In fact it can be shown to have no effect on large communities¹. Next, including correlations between species increases the diversity, to a degree that depends on the model parameters. To go beyond these results and find a sufficient condition for the community species to persist, we turn to the properties of the community interactions α^* at a given species abundance \vec{N}^* .

As was discussed above, interspecies interactions in the community are on average less competitive than those in the entire pool. When considered jointly with the species abundance², this change in interaction strength is not

¹ As was discussed above, at large S the distribution of α_{ij}^* has a different mean but the same variance as α_{ij} . To leading order in S the fraction of of persist species depends only on σ (when all $K_i = 1$), and changes in the distribution that alter $\mu \rightarrow \mu_{eff}$ have a sub-leading effect on the fraction of persistent species.

² In phase one (where the analytical theory is exact), the dynamics converge to stable equilibria, so that \vec{N}^* is a well-defined, time-independent quantity.

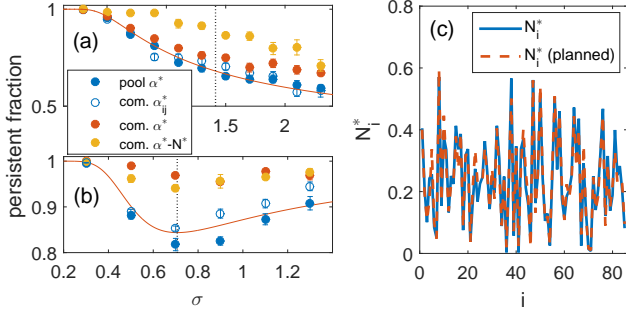


Figure 6. How different properties of the assembled network affect the number of species that persist, compared to an assembled community. (a,b) The fraction of persistent species in networks with different properties (for $\gamma = 0, 1$ respectively). When network parameters are sampled at random, as in the pool, only a fraction of the species persist. Sampling α_{ij}^* as in an assembled community does little to increase the persistence fraction. Adding correlations between interaction elements, as in Fig. 4, does increase the fraction in some cases. Consistently high diversity is obtained when correlations between species abundances and interactions are included. (c) These correlations are sufficient to reconstruct a given species abundance patterns. Model parameters: $\mu = 4$ with normally distributed α_{ij}^* . In (c), $\gamma = 0$ and $\sigma = 0.7$.

uniform, but depends the abundance of the species involved in the interaction. Specifically, the conditional distribution $\Pr(\alpha_{ij}^* | \vec{N}^*)$ has the same standard deviation as α_{ij} of the pool. Its mean, $\text{mean}_{\vec{N}^*}(\alpha_{ij}^*)$, is shifted with respect to the pool mean, and depends on N_i^* and N_j^* in a remarkably simple way:

$$\frac{\text{mean}_{\vec{N}^*}(\alpha_{ij}^*)}{\text{mean}(\alpha_{ij})} - 1 = -AN_i^*N_j^* + B(\gamma N_i^* + N_j^*) \quad , \quad (2)$$

with $A = (1/\mu + \gamma B \langle N \rangle) / \langle N^2 \rangle$ and $B = (1/\mu - \langle N \rangle) / \langle N^2 \rangle$, see Fig. 7. The correlation coefficient of $\alpha_{ij}^*, \alpha_{ik}^*$ conditioned on a given \vec{N}^* is given by $\text{corr}_{\vec{N}^*}(\alpha_{ij}^*, \alpha_{ik}^*) = -\frac{1}{S \langle N^2 \rangle} N_j^* N_k^*$. The other distinct correlations, $\text{corr}_{\vec{N}^*}(\alpha_{ij}^*, \alpha_{ki}^*)$ and $\text{corr}_{\vec{N}^*}(\alpha_{ji}^*, \alpha_{ki}^*)$ are given by the same expression, only multiplied by γ and γ^2 respectively. From Eq. (2) one finds that competition is always reduced when both abundances are large and $N_i^* > N_j^*$. Depending on model parameters, competition may increase for small N_i^* or N_j^* ; this is visible in Fig. 7(c). Expressions for a unequal carrying capacities are very similar, see Appendix A. We note in passing that following from these results, correlations between an interaction and the abundances of the species involved are always negative.

With these in mind, we generate communities by first sampling the species abundances (whose distribution is known exactly) and then sampling the matrix α^* at a given species abundance obeying Eq. (2) and the correlations following it. This produces communities where

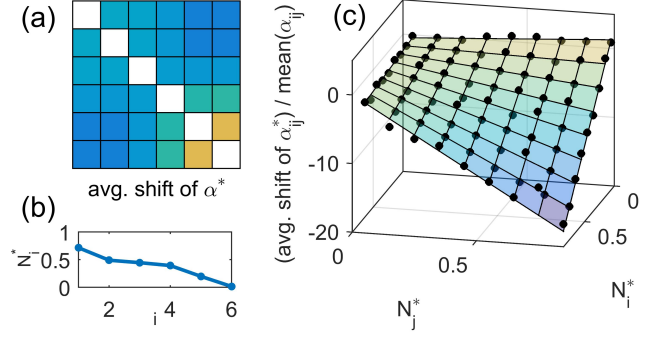


Figure 7. Interspecies interactions at a given species abundance are on average shifted, as shown in (a). The shift depends on the abundances (b), which are sorted for clarity. The bias is mostly, but not always, towards reduced competition. This pattern is responsible for species coexistence in the community. (c) Comparison of Eq. (2) with simulations. Model parameters: $\gamma = 0$, $\sigma = 1.1$ and $\mu = 4$.

almost all species persist, see Fig. 6(b,c). For large communities, this fraction will now be shown to go to one (at least in the unique equilibrium phase, where the theory is exact). The interactions α^* sampled in this way also satisfy all the properties that were described in the first part of the Results, and in fact can be derived from them. These relations therefore combine all community properties while maintaining almost complete diversity.

To understand why the species persist when sampled this way, we show that once the abundances \vec{N}^* have been chosen and α^* sampled on their basis, the dynamics will have a fixed point at \vec{N}^* , see the example in Fig. 6(c). To show this, note that for \vec{N}^* to be an equilibrium of Eq. (1), the quantity $I = 1 - N_i^* - \sum_{j, (j \neq i)} \alpha_{ij}^* N_j^*$ must vanish for all the persistent variables. Indeed, both the mean and variance of I at a given \vec{N}^* are zero: in the expectation value of I , α_{ij}^* is replaced by $\text{mean}_{\vec{N}^*}(\alpha_{ij}^*)$. Using Eq. (2) one obtains³

$$1 - \mu \langle N \rangle - \mu B \langle N^2 \rangle + (\mu A \langle N^2 \rangle - \mu B \gamma \langle N \rangle - 1) N_i^* \quad (3)$$

which is zero, using the definitions of A, B . A similar calculation using $\text{corr}_{\vec{N}^*}(\alpha_{ij}^*, \alpha_{ik}^*)$ given after Eq. (2) shows that the variance of I is also zero. And since the sampled abundances \vec{N}^* are chosen to be positive, the network admits a feasible solution. It is also stable, at least were the theory is exact, see the Discussion section below. This completes the argument for species persistence.

Referring to the species abundances when discussing the network structure might seem redundant, since the

³ Here population averages are replaced by moments, e.g. $\langle N \rangle = S^{-1} \sum_i N_i$, justified since correlations between abundances N_i^* are negligible at large S , see Appendix A. In addition terms of order $1/S$ have been dropped, as the expressions for A, B do not retain this level of accuracy.

abundances are given by solving $\alpha^* \vec{N}^* = \vec{K}^*$ (with $\alpha_{ii}^* = 1$). But the joint distribution of α^*, \vec{N}^* would translate to moments of all orders α^* , if written directly in terms of α^* and \vec{K}^* . Diversity depends on these more complicated correlations, involving the inverse of the matrix α^* .

The bi-linear dependence of $\text{mean}_{\vec{N}^*}(\alpha_{ij}^*)$ on N_i^* and N_j^* resembles the Hebbian learning rule for Hopfield neural networks, where a pattern to be memorized is a vector of binary variables $\vec{\xi}$. It is memorized by adding to the interaction strength a term proportional to $\xi_i \xi_j$. This similarity⁴ is intriguing in light of the very different mechanisms shaping the interaction strengths: in neural networks the strength of the connections is changed in the learning process. In contrast, the reduced α^* matrix is formed by keeping only the persistent species, rather than by modifying specific matrix entries. The interpretations are also different, as species abundance is viewed as a consequence of the assembly process, rather than an external input to be memorized.

II. DISCUSSION

What generates these properties – How do these patterns emerge from the community assembly process? It is quite intuitive that competition is on average reduced (Fig. 3): Species that suffer from less competition are more likely to persist, along with the interactions that involve these species. To estimate the strength of this effect, note that different values of α_{ij} change the probability that species i persists by an order of α_{ij} (more precisely by $\alpha_{ij} N_j \rho$, where ρ is the probability density of N_i at $N_i \rightarrow 0$). The shift in the mean interaction is roughly the typical size of α_{ij} weighted by the probability shifts, giving α_{ij}^2 or more precisely $\text{var}(\alpha_{ij})$. The mean and shifts in the mean are comparable even for large systems with many weak interactions, in accordance with Eq. (2), since at large S and fixed μ, σ , this variance σ^2/S is comparable to the mean μ/S .

More elaborate arguments can help to understand the signs of the correlations in Fig. 4. For example, consider the positive correlations between interactions sharing the same influencing species, Fig. 4(b). This is because a pair of interactions is less likely to be found in the community when the effect of one species on two others has opposing trends, causing one of the species to suffer from stronger competition which reduces its probability to per-

sist. These arguments are in essence Bayesian: from the probability that species persist given certain network patterns, one obtains the probability of finding these patterns given that the involved species persist.

Stability – Stability may be an important factor affecting the structure of communities [5, 32]. The main results of this paper follow from feasibility and resistance to invasion, without invoking (linear) stability. Conversely, this means that the results do not follow from requiring that a fixed-point be stable. Linear stability requires that the matrix $M_{ij}^* = -\alpha_{ij}^* \rho_i^* N_i^* / K_i^*$ be negative definite. This is generally the case in phase one (see Fig. 2), if \vec{r}^* is sampled independently from α^* and \vec{K}^* . This was tested for different distributions (including identical values, exponential, power-law and uniform distributions). Stability may play a role the second phase by selecting certain fixed-points over others.

Nestedness – The pattern of the mean of α^* at a given abundance \vec{N}^* , Eq. (2), has the following property: when the rows columns are sorted by increasing abundance, the strongest interactions concentrate in the upper left corner (close to the element α_{11}^*), as is visually clear in Fig. 7(a,c). Such a ‘nested’ pattern is commonly discussed in the context of bipartite ecological networks with binary entries, such as mutualistic networks [38], but can be used to describe any network [39]. The element-to-element variations around the mean might make it difficult to visually observe this pattern, compare Fig. 1(b), and quantitative measures for nestedness should be used. The relation between this phenomena and nestedness in other systems is an interesting direction for future research.

The predictions of the theory could be tested against experiments, if interaction strengths can be measured. A community assembly experiment would be preferable, as it allows to directly compare between the pool and the community. In systems where the interactions are generated by a specific mechanism, the interactions in the pool might have different statistics, and the calculations presented here could be carried out for these scenarios. Indeed, at the core of the analytical technique are objects (the desired quantities conditioned on persistence) which can be evaluated in a wide range of models (such as the models in [30, 40–42]), including explicit resource competition, sparse or otherwise distributed interactions, and interactions involving three or more species.

It is a pleasure to thank J. Friedman, J. Gore, M. Kardar, D. Kessler, P. Mehta, D. Rothman and M. Tikhonov for valuable discussions. The support of the Pappalardo Fellowship in Physics is gratefully acknowledged.

⁴ The closest analogy is to the symmetric Lotka-Volterra model, $\gamma = 1$. The dynamics in both models admit a Lyapunov function: $\frac{1}{2} \sum_i N_i \left(-\sum_j \alpha_{ij}^* N_j + 2 \right)$ for the Lotka-Volterra model

and $\frac{1}{2} \sum_{i,j} w_{ij} s_i s_j$ for the Hopfield model. And the patterns $\alpha_{ij}^* = \text{mean}_{\vec{N}^*}(\alpha_{ij}^*)$ and $w_{ij} \propto \xi_i \xi_j$ generate maxima at \vec{N}^* and $\vec{\xi}$ respectively of the corresponding Lyapunov functions.

-
- [1] U. Bastolla, M. A. Fortuna, A. Pascual-García, A. Ferrera, B. Luque, and J. Bascompte, *Nature* **458**, 1018 (2009).
- [2] J. A. Fuhrman, *Nature* **459**, 193 (2009).
- [3] R. M. Thompson *et. al.*, *Trends in Ecology & Evolution* **27**, 689 (2012).
- [4] R. May and A. McLean, *Theoretical Ecology: Principles and Applications* (Oxford University Press on Demand, 2007).
- [5] J. M. Montoya, S. L. Pimm, and R. V. Solé, *Nature* **442**, 259 (2006).
- [6] K. S. McCann, *Nature* **405**, 228 (2000).
- [7] K. McCann, A. Hastings, and G. R. Huxel, *Nature* **395**, 794 (1998).
- [8] R. H. MacArthur and E. O. Wilson, *Theory of Island Biogeography* (Princeton University Press, 2015).
- [9] M. A. Leibold *et. al.*, *Ecology Letters* **7**, 601 (2004).
- [10] A. Roberts, *Nature* **251**, 607 (1974).
- [11] U. Bastolla, M. Lässig, S. C. Manrubia, and A. Valleriani, *Journal of Theoretical Biology* **235**, 521 (2005).
- [12] R. P. Rohr, S. Saavedra, and J. Bascompte, *Science* **345**, 1253497 (2014).
- [13] C. K. Fisher and P. Mehta, *Proceedings of the National Academy of Sciences* **111**, 13111 (2014).
- [14] G. D. Kokkoris, A. Y. Troumbis, and J. H. Lawton, *Ecology Letters* **2**, 70 (1999).
- [15] M. E. Gilpin and T. J. Case, *Nature* **261**, 40 (1976).
- [16] S. Diederich and M. Opper, *Physical Review A* **39**, 4333 (1989).
- [17] J. A. Drake, *Journal of Theoretical Biology* **147**, 213 (1990).
- [18] W. M. Post and S. L. Pimm, *Mathematical Biosciences* **64**, 169 (1983).
- [19] T. J. Case, *Proceedings of the National Academy of Sciences* **87**, 9610 (1990).
- [20] R. Law and R. D. Morton, *Ecology* **77**, 762 (1996).
- [21] R. D. Morton and R. Law, *Journal of Theoretical Biology* **187**, 321 (1997).
- [22] J. A. Capitán, J. A. Cuesta, and J. Bascompte, *Physical Review Letters* **103**, (2009).
- [23] P. Biscari and G. Parisi, *Journal of Physics A: Mathematical and General* **28**, 4697 (1995).
- [24] D. A. Kessler and N. M. Shnerb, *Physical Review E* **91**, 42705 (2015).
- [25] Y. Fried, D. A. Kessler, and N. M. Shnerb, *arXiv:1605.07479* (2016).
- [26] H. Rieger, *Journal of Physics A: Mathematical and General* **22**, 3447 (1989).
- [27] M. Opper and S. Diederich, *Physical Review Letters* **69**, 1616 (1992).
- [28] K. Tokita, *Physical Review Letters* **93**, (2004).
- [29] K. Tokita, *Ecological Informatics* **1**, 315 (2006).
- [30] Y. Yoshino, T. Galla, and K. Tokita, *Physical Review E* **78**, (2008).
- [31] A. Goudard and M. Loreau, *The American Naturalist* **171**, 91 (2008).
- [32] R. M. May, *Nature* **238**, 413 (1972).
- [33] R. MacArthur and R. Levins, *American Naturalist* **377** (1967).
- [34] M. Mézard, G. Parisi, and M. A. Virasoro, *Europhys. Lett* **1**, 77 (1986).
- [35] A. Crisanti, H. Horner, and H.-J. Sommers, *Zeitschrift Für Physik B Condensed Matter* **92**, 257 (1993).
- [36] R. Paine, *Nature* **355**, 73 (1992).
- [37] A.-M. Neutel, J. A. Heesterbeek, and P. C. de Ruiter, *Science* **296**, 1120 (2002).
- [38] J. Bascompte, P. Jordano, C. J. Melián, and J. M. Olesen, *Proceedings of the National Academy of Sciences* **100**, 9383 (2003).
- [39] S. Jonhson, V. Domínguez-García, and M. A. Muñoz, *PloS One* **8**, e74025 (2013).
- [40] T. Galla, *Journal of Statistical Mechanics: Theory and Experiment* 2005, P11005 (2005).
- [41] T. Galla, *Journal of Physics A: Mathematical and General* **39**, 3853 (2006).
- [42] Y. Yoshino, T. Galla, and K. Tokita, *Journal of Statistical Mechanics: Theory and Experiment* 2007, P09003 (2007).
- [43] J. Hofbauer and K. Sigmund, *Evolutionary Games and Population Dynamics* (Cambridge university press, 1998).

Appendix A: Derivations

In this appendix all derivations of the results are given. First, the problem is set up and notation is defined. In the following section the species abundance is calculated, along with quantities that are used to study the network. This is followed by the distribution of carrying capacities, the distribution and correlations of community interspecies interactions, and correlations between carrying capacities and interactions.

1. Notation and model definition

Throughout, for random variable f, g , $P(f)$ is the probability distribution of f , $\langle f \rangle$ the mean, and $\text{var}(f) \equiv \langle f^2 \rangle - \langle f \rangle^2$, $\text{cov}(f, g) \equiv \langle fg \rangle - \langle f \rangle \langle g \rangle$, $\text{corr}(f, g) \equiv \text{cov}(f, g) / \sqrt{\text{var}(f) \text{var}(g)}$ the variance, covariance and correlation coefficients. The Gaussian distribution will be denoted by

$$g(x; \mu, \sigma^2) \equiv \frac{1}{\sqrt{2\pi\sigma}} e^{-\frac{1}{2\sigma^2}(x-\mu)^2}. \quad (\text{A1})$$

Similar notation, $g(\mathbf{x}; \mu, \Sigma)$, applies to multivariate distributions where μ, \mathbf{x} are vectors and Σ the covariance matrix.

The Lotka-Volterra equations with varying carrying capacities, Eq. (1), read

$$\frac{dN_i}{dt} = \frac{r_i}{K_i} N_i \left(K_i - N_i - \sum_{j, (j \neq i)} \alpha_{ij} N_j \right),$$

It will be convenient to work with variables a_{ij} defined by

$$\alpha_{ij} = \frac{\mu}{S} + \sigma a_{ij}, \quad (\text{A2})$$

with $\langle a_{ij} \rangle = 0$, $\langle a_{ij}^2 \rangle = 1/S$ and $\langle a_{ij} a_{ji} \rangle = \gamma/S$, so the relations for α_{ij} are satisfied. The carrying capacities K_i are sampled independently of the α_{ij} . By rescaling $N_i \rightarrow N_i / \langle K_i \rangle$, we set $\langle K_i \rangle = 1$. It will be convenient to take the K_i to be Gaussian with unit mean and $\sigma_K^2 \equiv \text{var}(K_i)$. Since the K_i must be positive, this is reasonable for $\sigma_K \lesssim 0.3$. The calculations can be carried out for other distributions of carrying capacities.

Fixed points $dN_i/dt = 0$ for all i require $N_i (K_i - N_i - \sum_{j \neq i} \alpha_{ij} N_j) = 0$. Using the definition of a_{ij} and rearranging this becomes

$$0 = n_i \left(\lambda_i - un_i - \sum_{j \neq i} a_{ij} n_j + h \right), \quad (\text{A3})$$

where n_i are the normalized abundances

$$n_i = N_i / \left(\frac{1}{S} \sum_{j=1}^S N_j \right)$$

so that $\frac{1}{S} \sum_{i=1}^S n_i = 1$, and

$$u = \frac{1 - \mu/S}{\sigma}, \quad \lambda_i = \frac{K_i - 1}{\sigma \langle N \rangle}, \quad h = \frac{1/\langle N \rangle - \mu}{\sigma}. \quad (\text{A4})$$

From this equation it follows that $\langle \lambda_i \rangle = 0$ and $\sigma_\lambda^2 \equiv \langle \lambda_i^2 \rangle = \sigma_K^2 / (\sigma \langle N \rangle)^2$. In this language the problem becomes: given u and σ_λ^2 , find a value of h such that: Eq. (A3) holds for all species; $\sum_{i=1}^S n_i = S$; species for which $n_i = 0$ cannot invade ($dN_i/dt < 0$ for small N_i); and the persistent species ($n_i > 0$) are stable against small perturbations in n_i . At large S , $u \simeq 1/\sigma$ to lowest order in $1/S$, which is used throughout the paper in comparisons with Lotka-Volterra simulations. The exact form $(1 - \mu/S)/\sigma$ can be used if one is interested in the behavior close to the Hubble point [24] $\mu/S = \text{mean}(\alpha_{ij}) = 1$.

The form used in Eq. (A3) has a number of advantages. First, it is more convenient to work with zero mean and standardized variance a_{ij} variables. Secondly, a connection to the Replicator Equation is established, as the fixed points of Eq. (A3) are precisely those of the Replicator Equations $dn_i/dt = n_i (\lambda_i - un_i - \sum_{j \neq i} a_{ij} n_j + h)$ and the connection is made to works that study its properties, such as species abundance or the existence of multiple equilibria⁵. Perhaps most importantly, as Eq. (A3) depends on the original parameters only through the combinations in Eq. (A4), new relations are revealed. For example, if all carrying capacities are identical ($K_i = 1$), then $\sigma_\lambda^2 = 0$ and the problem depends on all the original parameters through u , equal to $1/\sigma$ at large S . Therefore all properties of the normalized abundances n_i do not depend on μ , see Fig. 8(a,c). This applies to all properties of the reduced matrix, whose structure is determined by which n_i are positive.

Summary of notation – The set of persistent variables, for which $N_i > 0$, are denoted by N_i^* , and similarly $K_i^*, n_i^*, \lambda_i^*$. S^* will denote the size of the community (number of persistent variables). The community (or reduced) interaction matrix is α^* , containing all interactions α_{ij} for which $N_i, N_j > 0$. The fraction of persistent variables and the second moment will be denoted by

$$\phi \equiv S^*/S \quad ; \quad q \equiv \langle n_i^2 \rangle.$$

Note that the average in q also includes species for which $n_i = 0$. The correlations between abundances n_i for different species are weak (as shown below), and S^* fluctuations will be of order $\sqrt{S^*}$, so at large S , ϕ can be replaced with its mean value. Similarly, $\sum_i n_i^k / S$ can be replaced with $\langle n_i^k \rangle$.

⁵ The mapping in Eq. (A3) only holds for the equilibrium properties. It is *not* the well-known mapping of the full dynamics [28, 43], which requires changing variables in a way that generates statistical dependencies between interactions, even if they don't exist in the original Lotka-Volterra equations.

Because $n_i = 0$ for species outside the community, $\sum_{i'} n_{i'}^* = \sum_i n_i = S$, therefore

$$\langle n_i^* \rangle = \sum_j n_j^* / S^* = 1/\phi,$$

and similarly

$$\langle (n_i^*)^2 \rangle = q/\phi.$$

It will be useful to consider the change in a solution n_i to Eq. (A3) as the λ_i are varied,

$$v \equiv \left\langle \frac{\partial n_i}{\partial \lambda_i} \right\rangle$$

and use the shorthand notation

$$\hat{u} \equiv u - \gamma v.$$

2. Species abundance distribution

Here a variant of the cavity method [16, 26, 27, 34, 35] is used. It is based on the dynamical cavity method [26, 27], which does not require α_{ij} to be symmetric, but replaces its generating functional formalism by a more elementary derivation, close in spirit to [34]. It proceeds by adding a new species along with newly sampled interactions with the existing system, and comparing the properties of the solution with S species to that with $S+1$ species, requiring that the new species has the same properties as the rest.

Assume that the abundances $n_{i \setminus 0}$ of the species in the pool $i = 1..S$ are known. Introduce a new species with interactions $\{a_{0i}, a_{i0}\}_{i=1..S}$ and λ_0 . For the purposes of the derivation, Eq. (A3) is extended to include an additional small perturbation ξ_i to the λ_i of each species, later set to zero:

$$0 = n_i \left(\lambda_i - u n_i - \sum_{j \neq i} a_{ij} n_j + h + \xi_i \right) \quad (\text{A5})$$

and the response to the perturbation is

$$v_{ij} \equiv [\partial n_i / \partial \xi_j]_{\xi_j=0}. \quad (\text{A6})$$

Once the new species is introduced, it might invade and its final abundance will be $n_0 > 0$, or else $n_0 = 0$. The effect it has on the species $i \geq 1$ is⁶

$$u n_i = \lambda_i - \sum_{j \neq i} a_{ij} n_j + h - a_{i0} n_0$$

⁶ Here we assume that $v_{ij} = 0$ if $n_i = 0$. A small fraction, of order $1/\sqrt{S}$, of the species with $n_{j \setminus 0}$ may acquire a positive abundance of order $1/\sqrt{S}$, but this effect is negligible.

This is the same as Eq. (A5), with $\xi_i = -a_{i0} n_0$. For large S each $a_{i0} n_0$ is small (scales as $1/\sqrt{S}$) so that linear response can be used, $n_j = n_{j \setminus 0} - \sum_k v_{jk} \xi_k$, giving

$$n_j = n_{j \setminus 0} - n_0 \sum_k v_{jk} a_{k0}.$$

If $n_0 > 0$ we substitute this equation into $0 = \lambda_0 - u n_0 - \sum_j a_{0j} n_j + h + \xi_0$ and rearrange to find that $n_0 = n_0^+$, where

$$n_0^+ \equiv \frac{\lambda_0 - \sum_j a_{0j} n_{j \setminus 0} + h + \xi_0}{u - \sum_{j,k} v_{jk} a_{0j} a_{k0}} \quad (\text{A7})$$

The denominator of this equation will be a finite number with negligible fluctuations. To see this, note that $v_{ii} = O(S^0)$, while v_{ij} which is mediated by the a interactions is expected to be $v_{ij} = O(S^{-1/2})$ (as can be verified later⁷). The sum over the $j = k$ terms in $\sum_{j,k} v_{jk} a_{0j} a_{k0}$ gives

$$\left\langle \sum_j v_{jj} a_{0j} a_{j0} \right\rangle = \sum_j v_{jj} \langle a_{0j} a_{j0} \rangle = \frac{\gamma}{S} \sum_j v_{jj}$$

with $O(S^{-1/2})$ fluctuations, while the sum over the $j \neq k$ terms is $O(S^{-1/2})$. Together, up to $O(S^{-1/2})$ fluctuations, the denominator is equal to $u - \gamma v$ with $v \equiv \langle v_{jj} \rangle$. All in all, the feedback of the existing species on the new species changes the denominator from u to $u - \gamma v$.

Turning to the numerator of Eq. (A7), the term $\lambda_0 - \sum_j a_{0j} n_{j \setminus 0} + h$ has mean h and variance $\sigma_\lambda^2 + \sum_j \langle a_{0j}^2 \rangle \langle n^2 \rangle = \sigma_\lambda^2 + q$ where $q \equiv \langle n^2 \rangle$. This follows from the distributions of λ_0 and a_{0j} (all independent from each other by construction). As a sum of many weakly correlated terms $-\sum_j a_{0j} n_{j \setminus 0}$ is Gaussian (see e.g. [?]), and so the numerator is Gaussian, $h + \xi_0 + \sqrt{q + \sigma_\lambda^2} z$ with $P(z) = g(z; 0, 1)$. Setting $\xi_0 = 0$, Eq. (A7) becomes

$$n_0^+ = \frac{1}{u - \gamma v} \left(h + \sqrt{q + \sigma_\lambda^2} z \right). \quad (\text{A8})$$

From the Lotka-Volterra equations, Eq. (1), it follows that if $n_0^+ > 0$, the solution $n_0 = 0$ is not stable against invasion ($dN_0/dt > 0$ at $N_0 \rightarrow 0^+$), so $n_0 = n_0^+$. This is where the resistance to invasion enters. Together $n_0 = \max(0, n_0^+)$ with n_0^+ given in Eq. (A8). But once species ‘0’ has been added to the system it is in no way different

⁷ From the definition of v_{ij} , Eq. (A6), the change δn_i in response to a perturbation vector $\vec{\xi}$ is $\delta n_i = \sum_j v_{ij} \xi_j$. If the elements of $\vec{\xi}$ are sampled independently then $\langle (\delta n)^2 \rangle / \langle \xi^2 \rangle = v^2 + (S-1) \langle v_{ij}^2 \rangle$. As long as this is finite, as discussed in B, v_{ij} scales as $1/\sqrt{S}$.

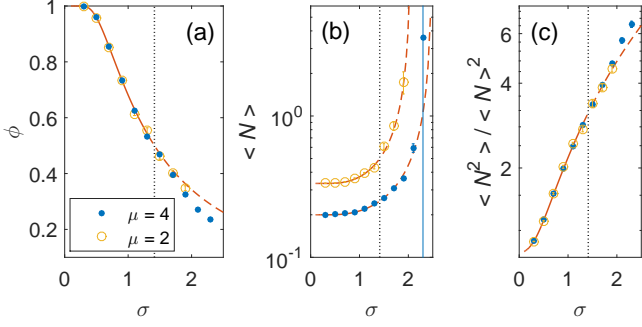


Figure 8. Properties of species abundance, for $\gamma = 0$, $\mu = 2, 4$ and $\sigma_K^2 = 0$. ϕ is the fraction of persistent species. Solid and dashed line are analytical predictions, exact in the unique equilibrium phase, left of the vertical dotted line.

from the other species, so we may drop the subscript ‘0’ to obtain the species abundance distribution of all species,

$$n = \max\left(0, \frac{h + \sqrt{q + \sigma_\lambda^2 z}}{u - \gamma v}\right). \quad (\text{A9})$$

The distribution of n is therefore a truncated Gaussian.

It remains to find the values of q, v, h, ϕ . Using Eq. (A9) for n , the relations $1 = \langle n \rangle$, $q = \langle n^2 \rangle$, $\phi = \langle \Theta^+(n) \rangle$ can be used. $\phi = \langle \Theta^+(n) \rangle$ is the fraction of persistent species, and $\Theta^+(n) = 0$ if $n < 0$ and 1 otherwise. Denoting $w_k(\Delta) \equiv \int_{-\Delta}^{\infty} \frac{1}{\sqrt{2\pi}} e^{-\frac{z^2}{2}} (z + \Delta)^k dz$, these relations read

$$\begin{aligned} v(u - \gamma v) &= w_0(\Delta) \\ u - \gamma v &= \sqrt{q + \sigma_\lambda^2} w_1(\Delta) \\ (u - \gamma v)^2 &= (1 + \sigma_\lambda^2/q) w_2(\Delta) \end{aligned} \quad (\text{A10})$$

where $\Delta \equiv h/\sqrt{q + \sigma_\lambda^2}$. A fourth equation is obtained by differentiating Eq. (A7) with respect to ξ_0 : if $n_0 > 0$ it gives $v_{00} = 1/(u - \gamma v)$ and otherwise $v_{00} = 0$. Together

$$v = \langle v_{00} \rangle = \phi \frac{1}{u - \gamma v}. \quad (\text{A11})$$

This completes the set of four coupled equations for the unknowns q, v, h, ϕ . Using the identity $w_2(\Delta) = w_0(\Delta) + \Delta \cdot w_1(\Delta)$ and the definition of Δ , we also have

$$h = q [u - v (1 + \gamma + \sigma_\lambda^2/q)]. \quad (\text{A12})$$

These equations were first derived, for $\sigma_\lambda^2 = 0$, in the context of the Replicator Equations in [16, 27]. They can be solved numerically by evaluating $q = w_2/w_1^2$, $v = w_0/(w_1\sqrt{q + \sigma_\lambda^2})$ and $u = \gamma v + \sqrt{q + \sigma_\lambda^2} w_1$ as functions of Δ and σ_λ^2 , and then plotting the different quantities against each other.

Returning to the Lotka-Volterra variables $N_i = \langle N \rangle n_i$, one has $\langle N \rangle = \sigma h + \mu$ from Eq. (A4) and $\langle N^2 \rangle =$

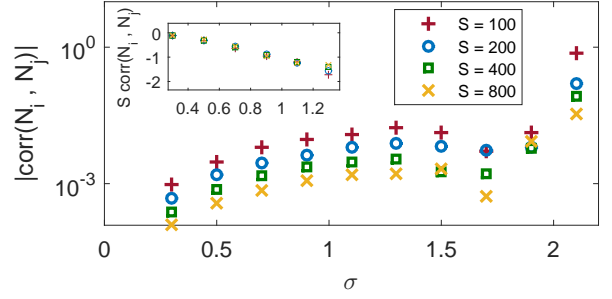


Figure 9. Correlation between abundances. Inset: In phase one, the correlation for different S collapse when multiplied by S .

$q \langle N \rangle^2 = q(\sigma h + \mu)^2$. The species abundance of N_i is a truncated Gaussian from Eq. (A9), fully characterized by $\langle N \rangle$ and $\langle N^2 \rangle$. Fig. 8 shows the fraction of persistent variables and the moments $\langle N \rangle$ and $\langle N^2 \rangle$ and the species abundance distribution, for $\gamma = 0$, $\sigma_K^2 = 0$ and $\mu = 2, 4$. Those are compared with numerical simulations at large S (the simulations are described in Sec. D. Small S values are discussed in Sec. C). The analytical results are exact phase one, where a unique equilibrium exists (left of the vertical dotted line), but serve as a good approximation beyond that. Note also that the quantities in Fig. 8(a,c), which are properties of the normalized abundances n_i alone, give the same result for both $\mu = 2$ and 4, as was discussed in Sec. A 1. The correlations between abundances are weak and higher order in $1/S$, see Fig. 9. Their precise form will not be needed in the following.

3. Carrying capacity distribution of persistent community

As a first calculation of a property of the community network, the distribution of carrying capacity in persistent community is derived. It will turn out to have higher average values and lower variance in the community as compared the entire species pool, see Fig. 5 in the main text.

As in the previous section, see Eq. (A8), $n_0 = \max(0, n_0^+)$ with

$$n_0^+ = \frac{1}{\hat{u}} (\lambda_0 + \eta_0 + h).$$

Here $\eta_0 \equiv -\sum_j a_{0j} n_{j\lambda_0}$ and $\hat{u} \equiv u - \gamma v$. Recall that $P(\lambda_0) = g(\lambda_0; 0, \sigma_\lambda^2)$, $P(\eta_0) = g(\eta_0; 0, q)$ and $P(\lambda_0, \eta_0) = P(\lambda_0) P(\eta_0)$. We now wish to obtain the joint probability of λ_0, n_0^+ , restricted to $n_0^+ > 0$, see Fig. 10. First, changing variables $(\lambda_0, \eta_0) \rightarrow (\lambda_0, n_0^+)$,

$$\begin{aligned} P(\lambda_0, n_0^+) &= \left| \frac{\partial \eta_0}{\partial n_0^+} \right| P(\lambda_0, \eta_0) \\ &= |\hat{u}| g(\lambda_0; 0, \sigma_\lambda^2) g(\hat{u} n_0^+ - \lambda_0; h, q). \end{aligned}$$

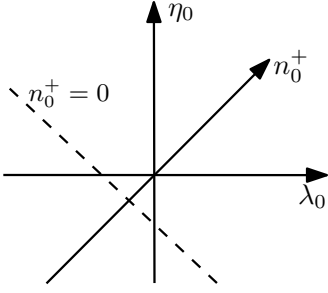


Figure 10. λ_0 is the rescaled carrying capacity of the added species 0, η_0 the accumulated effect of interspecies interactions, and n_0 is the normalized abundance. λ_0 and η_0 are independent random variables, from which the joint distribution of λ_0 and n_0 is calculated, in the region where $n_0 = n_0^+ > 0$.

where $g(\cdot)$ is the normal distribution, see Eq. (A1). Rearranging we find

$$\begin{aligned} P(\lambda_0, n_0^+) &= \frac{|\hat{u}|}{2\pi\sigma_\lambda\sqrt{q}} e^{-\frac{1}{2}\left[\frac{\lambda_0^2}{\sigma_\lambda^2} + \frac{1}{q}(\hat{u}n_0^+ - \lambda_0 - h)^2\right]} \\ &= g\left(\lambda_0; \frac{\hat{u}n_0^+ - h}{1 + q/\sigma_\lambda^2}, \frac{q}{1 + q/\sigma_\lambda^2}\right) P(n_0^+) \end{aligned}$$

where recall from the previous section that $P(n_0^+) = g\left(n_0^+; \frac{h}{\hat{u}}, \frac{q+\sigma_\lambda^2}{\hat{u}^2}\right)$. Since $P(\lambda_0, n_0^+) = P(\lambda_0|n_0^+) P(n_0^+)$, the first term in the second line is $P(\lambda_0|n_0^+)$. Now, restricting the distribution to $n_0 > 0$, the distributions $P_{n_0^+>0}(\lambda_0, n_0^+)$, $P_{n_0^+>0}(n_0^+)$ change only their normalization, and $P(\lambda_0|n_0^+)$ remains unchanged. Also, $n_0 = n_0^+$ when restricted to $n_0 > 0$, and moreover this species is not different from any other in the community, so $P(\lambda_i^*, n_i^*) = P_{n_0>0}(\lambda_0, n_0^+)$ for any persistent i :

$$P(\lambda_i^*|n_i^*) = g\left(\lambda_i^*; \frac{\hat{u}n_i^* - h}{1 + q/\sigma_\lambda^2}, \frac{q}{1 + q/\sigma_\lambda^2}\right). \quad (\text{A13})$$

The mean of λ_i^* shifts when conditioned to n_i^* , and the variance of $P(\lambda_i^*|n_i^*)$ is not affected by n_i^* . An advantage of the conditional expression is that moments can be easily calculated. As $\int_{-\infty}^{\infty} d\lambda_i^* P(\lambda_i^*|n_i^*) \lambda_i^* = \frac{\hat{u}n_i^* - h}{1 + q/\sigma_\lambda^2}$, integrating this over $\int_{0^+}^{\infty} dn_i^* P(n_i^*)$ and using $\langle n_i^* \rangle = 1/\phi$ (see Sec. A 1) the average reads

$$\langle \lambda_i^* \rangle = \frac{\hat{u}/\phi - h}{1 + q/\sigma_\lambda^2}, \quad (\text{A14})$$

and by $\int_{-\infty}^{\infty} d\lambda_i^* P(\lambda_i^*|n_i^*) (\lambda_i^*)^2 = \left(\frac{\hat{u}n_i^* - h}{1 + q/\sigma_\lambda^2}\right)^2 + \frac{q}{1 + q/\sigma_\lambda^2}$, $\langle (n_i^*)^2 \rangle = q/\phi$ and $\langle n_i^* \rangle = 1/\phi$,

$$\text{var}(\lambda_i^*) = \hat{u}^2 \frac{q/\phi - 1/\phi^2}{(1 + q/\sigma_\lambda^2)^2} + \frac{q}{1 + q/\sigma_\lambda^2}. \quad (\text{A15})$$

Finally, note that the distribution $P(\lambda_i^*)$ is precisely that of λ_0 when $n_0^+ > 0$. Integrating Eq. (A13) over

$n_0^+ > 0$ gives

$$P(\lambda_i^*) = g(\lambda_i^*; 0, \sigma_\lambda^2) \frac{1}{2} \left[1 + \text{sign}(\hat{u}) \text{erf} \frac{\lambda_i^* + h}{\sqrt{2q}} \right]. \quad (\text{A16})$$

The expressions for the moments, Eqs. (A14,A15), could have been obtained by integrating $P(\lambda_i^*)$ and relating the results to terms in Eq. (A10). It was more convenient to use the conditional probability since $\langle (n_i^*)^2 \rangle$ and $\langle n_i^* \rangle$ are given directly in terms of ϕ, q .

The distribution of the persistent carrying capacities, $P(K_i^*)$ and its moments can be readily deduced from $\lambda_i = \frac{K_i - 1}{\sigma\langle N \rangle}$, see Eq. (A4). Thus $\langle K_i^* \rangle = 1 + \sigma\langle N \rangle \langle \lambda_i^* \rangle$ and $\text{var}(K_i^*) = \frac{1}{\sigma^2\langle N \rangle^2} \text{var}(K_i^*)$. Fig. 5 shows $P(K_i^*)$ and the moments for one set of model parameters. The mean satisfies $\langle K_i^* \rangle > \langle K_i \rangle = 1$ always, since up to a normalization $P(\lambda_i^*)$ is equal to $P(\lambda_i)$ multiplied by an increasing function. For a Gaussian distribution of K_i , $\text{var}(K_i^*) < \text{var}(K_i)$ (this was verified by evaluating Eq. (A15) over a wide range of μ, σ_K , for $-1 \leq \gamma \leq 1$ and σ up to the unbounded growth phase). However this will not hold for any distribution. For example, if $P(K_i)$ is bi-modal, where most of the probability is in a low and narrow part, and a smaller part is higher and wide. If $P(K_i^*)$ contains mostly the top part, then it may have a larger variance than $P(K_i)$ ⁸

4. Distribution of α_{ij}^*

In this section the distribution of a single element in α_{ij}^* is derived. Since by definition, $P(\alpha_{ij}^*) = P(\alpha_{ij}^*|n_i, n_j > 0)$, this conditional distribution is calculated. The derivation follows a path similar to the previous section, but now introducing two new species at once, denoted $i = 1, 2$ with abundance $n_{1,2}$. Define

$$\tilde{h}_k \equiv \lambda_k - \sum_{j \notin \{1,2\}} a_{kj} n_j + h,$$

Its mean and variance are $\langle \tilde{h}_n \rangle = h$ and $\langle \tilde{h}_n^2 \rangle - \langle \tilde{h}_n \rangle^2 = q + \sigma_\lambda^2$. Following the same steps as in Sec. A 2, one finds that if both $n_1, n_2 > 0$ then $n_{1,2} = n_{1,2}^+$ where

$$\begin{aligned} \hat{u}n_1^+ &= \tilde{h}_1 + a_{12}n_2^+ \\ \hat{u}n_2^+ &= \tilde{h}_2 + a_{21}n_1^+ \end{aligned} \quad (\text{A17})$$

Where a_{12}, a_{21} satisfy $\langle a_{12}^2 \rangle = \langle a_{21}^2 \rangle = 1/S$ and $\langle a_{12}a_{21} \rangle = \gamma/S$.

⁸ As a proof of existence, consider a pool with 7 species: five species with $K = 0.05$, one with $K = 1$ and one with $K = 4$. All $\alpha_{ij} = 0.2$. Only the species with $K = 1, 4$ will persist, and the variance of the carrying capacities will be larger in the community.

Following similar steps to Sec. A 3, $P(a_{12}, a_{21}, n_1^+, n_2^+)$ is first calculated. As

$$P(a_{12}, a_{21}, \tilde{h}_1, \tilde{h}_2) = P(a_{12}, a_{21}) P(\tilde{h}_1) P(\tilde{h}_2),$$

$$P(a_{12}, a_{21}, n_1^+, n_2^+) = JP(a_{12}, a_{21}) P(\tilde{h}_1) P(\tilde{h}_2), \quad (\text{A18})$$

and \tilde{h}_1, \tilde{h}_2 are substituted by their values from Eq. (A17)

$$\begin{aligned} \tilde{h}_1 &= \hat{u}n_1^+ + a_{12}n_2^+, \\ \tilde{h}_2 &= \hat{u}n_2^+ + a_{21}n_1^+. \end{aligned}$$

J is the Jacobian of the change of variables $(a_{12}, a_{21}, \tilde{h}_1, \tilde{h}_2) \rightarrow (a_{12}, a_{21}, n_1^+, n_2^+)$,

$$J = \frac{1}{\hat{u}} - \frac{1}{\hat{u}^3} a_{12} a_{21}.$$

We now expand $P(\tilde{h}_{1,2})$ in the parameters a_{12}, a_{21} , since once the moments of the equation are taken below, higher powers of a_{ij} will give higher powers in $1/S$. Expanding to first order, $P(\tilde{h}_1) = g(\hat{u}n_1^+ - a_{12}n_2^+; h, \hat{q})$ becomes

$$\begin{aligned} P(\tilde{h}_1) &= g(\hat{u}n_1^+; h, q + \sigma_\lambda^2) - a_{12}n_2^+ g'(\hat{u}n_1^+; h, q + \sigma_\lambda^2) \\ &= \frac{1}{\hat{u}} P(n_1^+) \left[1 - \frac{a_{12}}{q + \sigma_\lambda^2} n_2^+ (\hat{u}n_1^+ - h) \right] \end{aligned}$$

where $P(n_1^+) = g(n_1^+; h/\hat{u}, (q + \sigma_\lambda^2)/\hat{u})$, see Eq. (A8).

Now $P(a_{12}, a_{21} | n_1^+, n_2^+) \propto P(a_{12}, a_{21}, n_1^+, n_2^+)$, where the proportionality includes all factors that are independent of $a_{12,21}$. Also, if both species are included in the community, $n_1, n_2 > 0$, then $n_i^+ = n_i^*$. To lowest order, from Eq. (A18)

$$\begin{aligned} P(a_{12}, a_{21} | n_1^*, n_2^*) &= \\ P(a_{12}, a_{21}) &\left[1 - \hat{u} \frac{a_{12} + a_{21}}{q + \sigma_\lambda^2} n_1^* n_2^* + h \frac{a_{12} n_2^* + a_{21} n_1^*}{q + \sigma_\lambda^2} \right]. \end{aligned} \quad (\text{A19})$$

This distribution is normalized when integrated over $a_{12,21}$ since $\langle a_{12} \rangle = \langle a_{21} \rangle = 0$. Using $\langle a_{12}^2 \rangle = 1/S$ and $\langle a_{12} a_{21} \rangle = \gamma/S$, the expectation value of a_{12} reads

$$\text{mean}_{n_1^*, 2} a_{12} = -\frac{(1 + \gamma) \hat{u} n_1^* n_2^* - h(\gamma n_1^* + n_2^*)}{S(q + \sigma_\lambda^2)}. \quad (\text{A20})$$

and $\text{mean}_{n_1^*, 2} a_{12}$ is similar, only with $1 \leftrightarrow 2$ indices switched. Corrections to this expression are $O(1/S^2)$. The variance and correlation are unchanged by the conditioning: $\text{var}_{n_1^*, 2} a_{12} = 1/S$, and $\text{corr}_{n_1^*, 2}(a_{12}, a_{21}) = \gamma$.

Going back to α_{ij} , using $\alpha_{ij} = \mu/S + \sigma a_{ij}$ together with $n_i = N_i / \sum_{j=1}^S N_j$ and the definitions of u, h, q in Eqs. (A4, A12) we find Eq. (2)

$$\frac{\text{mean}_{\bar{N}^*}(\alpha_{ij}^*)}{\text{mean}(\alpha_{ij})} - 1 = -AN_i^* N_j^* + B(\gamma N_i^* + N_j^*),$$

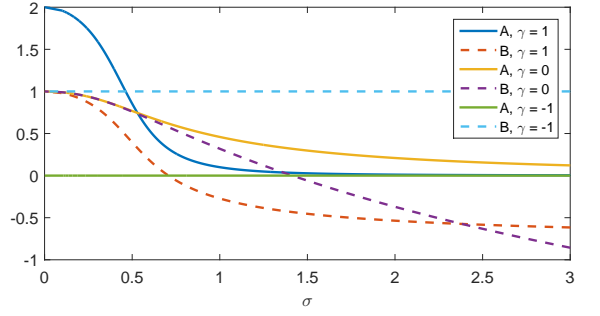


Figure 11. The functions A and B in Eq. (A21) as functions of σ , for $\gamma = -1, 0, 1$. Here all $K_i = 1$, and the function μA and μB are plotted, since in this case they do not depend on μ .

with A, B given by

$$\begin{aligned} B &= \frac{1/\mu - \langle N \rangle}{\langle N^2 \rangle + \sigma_K^2 / \sigma^2} \\ A &= \frac{(1 + \gamma)(1/\mu + \gamma \langle N \rangle B)}{\langle N^2 \rangle (1 + \gamma) + \sigma_K^2 / \sigma^2} \end{aligned} \quad (\text{A21})$$

These reduce to the expressions for A, B following Eq. 2 in the main text when $\sigma_{K/\bar{K}}^2 = 0, \bar{K} = 1$. A, B are plotted for different γ in Fig. 11. Note that A must vanish for $\gamma = -1$, as indeed can be seen in the figure, since it creates a shift of a_{ij} which is symmetric in N_i^*, N_j^* .

The mean of α_{ij}^* , plotted in Fig. 3, is

$$\begin{aligned} \langle \alpha_{ij}^* \rangle &= \int_{0+}^{\infty} dN_i^* P(N_i^*) \Delta \alpha_{ij}^* \\ &= -\frac{1}{S} [A \langle N_i^* N_j^* \rangle - B(\gamma \langle N_i^* \rangle + \langle N_j^* \rangle)] \end{aligned} \quad (\text{A22})$$

and $\langle N_i^* \rangle = \langle N_j^* \rangle = \langle N_i \rangle / \phi$ and $\langle N_i^* N_j^* \rangle = \langle N_i^* \rangle^2 + O(1/S) = \langle N \rangle^2 / \phi^2$ with $\langle N_i \rangle = \sigma h + \mu$ from Eq. (A4) can be used.

Finally, the distribution of a single element a_{12} can be readily derived from Eq. (A19). Integrating over a_{12} weighted by its distribution $P(a_{12})$, and using $\langle a_{12} \rangle = 0$, and then over $n_{1,2}^* > 0$ and using $\langle n_i^* \rangle = 1/\phi$ one finds $\text{Pr}(a_{12}^* = a) / \text{Pr}(a_{12} = a) = 1 - c \cdot a$, with

$$c = \frac{\hat{u}/\varphi - h}{(q + \sigma_\lambda^2)\varphi}.$$

This equation also holds for $\alpha_{ij}, \alpha_{ij}^*$ since $\text{Pr}(a_{12}^* = a) / \text{Pr}(a_{12} = a) = \text{Pr}(\alpha_{12}^* = \alpha) / \text{Pr}(\alpha_{12} = \alpha)$ when α, a are related as usual by Eq. (A2).

5. Two-element distributions

In this section the joint distribution of two elements, α_{ij}^* and α_{kl}^* is calculated. The correlation of α_{ij}^* with α_{kl}^*

is (to lowest order) the symmetry parameter γ , as was shown in the previous section. To order $1/S^2$, the only other non-zero correlations are along rows or columns of the matrix, i.e., when the pairs (i, j) and (k, l) share a single index.

$$\begin{aligned}\hat{u}n_1^+ &= \tilde{h}_1 - a_{12}n_2^+ - a_{13}n_3^+ \\ \hat{u}n_2^+ &= \tilde{h}_2 - a_{21}n_1^+ - a_{23}n_3^+ \\ \hat{u}n_3^+ &= \tilde{h}_3 - a_{31}n_1^+ - a_{32}n_2^+\end{aligned}\quad (\text{A23})$$

The list of the 6 interactions appearing will be denoted by $\{a_{ij}\}$, and the list $\{n_1^+, n_2^+, n_3^+\}$ by $\{n_i^+\}$. As before, the goal is to calculate the conditional $P(\{a_{ij}\} | \{n_i\})$, and the same path is followed: first, the joint distribution

$$P(\{a_{ij}\}, \{n_i^+\}) = JP(\{a_{ij}\})P(\tilde{h}_1)P(\tilde{h}_2)P(\tilde{h}_3)$$

is calculated, where the Jacobian is

$$J = \frac{1}{\hat{u}} - \frac{a_{12}a_{21} + a_{13}a_{31} + a_{23}a_{32}}{\hat{u}^3}$$

and $\tilde{h}_{1,2,3}$ are substituted by their values from Eq. (A23). Expanding $P(\tilde{h}_1)$ to second order in a_{ij} ,

$$P(\tilde{h}_1) = P(n_1^+) \left[1 - \frac{h - \hat{u}n_1^+}{q + \sigma_\lambda^2} \omega_{123} + \frac{(h - \hat{u}n_1^+)^2 - q - \sigma_\lambda^2}{2(q + \sigma_\lambda^2)^2} \omega_{123}^2 \right]$$

where $\omega_{123} \equiv a_{12}n_2^+ + a_{13}n_3^+$. Expanding $P(\{a_{ij}\} | \{n_i^+\}) \propto P(\{a_{ij}\}, \{n_i^+\})$ to $O(a_{ij}^2)$,

$$P(\{a_{ij}\} | \{n_i^+\}) \propto P(\{a_{ij}\}) [1 + (\dots)]$$

where the terms (\dots) in the brackets are first and second powers of $\{a_{ij}\}$. The different moments can now be calculated, remembering to divide by the normalization that is not trivial to $O(a_{ij}^2)$. The cross-correlations are

$$\begin{aligned}\text{corr}_{n_{1,2,3}^*}(a_{12}, a_{13}) &= -\frac{n_2^* n_3^*}{S^2 (q + \sigma_\lambda^2)} \\ \text{corr}_{n_{1,2,3}^*}(a_{12}, a_{31}) &= -\frac{\gamma n_2^* n_3^*}{S^2 (q + \sigma_\lambda^2)} \\ \text{corr}_{n_{1,2,3}^*}(a_{21}, a_{31}) &= -\frac{\gamma^2 n_2^* n_3^*}{S^2 (q + \sigma_\lambda^2)}\end{aligned}$$

These results require that the third moments $\mu_3 = \langle a_{ij}^3 \rangle$ decay faster than $O(1/S)$, since they generate a correction of order μ_3/S . This is rather mild: if one rescales a given distribution, $P(a_{ij}) = Sf(Sa_{ij})$, then $\mu_3 = O(S^{-3/2})$.

Going back to variables α_{ij} and N_i , $n_2^* n_3^* = N_2^* N_3^* / \langle N \rangle^2$ and $q + \sigma_\lambda^2 = \langle N^2 \rangle / \langle N \rangle^2 + \sigma_K^2 / \sigma^2$. For $\sigma_K = 0$ these become the relations in and following Eq. 2. The correlations over α^* shown in Fig. 4, are obtained

by integrating the above relations over $n_{1,2,3} > 0$. For example,

$$\begin{aligned}\langle \alpha_{12}^* \alpha_{23}^* \rangle - \langle \alpha_{12}^* \rangle^2 &= \sigma^2 \left(\langle a_{12}^* a_{23}^* \rangle - \langle a_{12}^* \rangle^2 \right) \\ &= -\frac{\sigma^2}{S^2 (q + \sigma_\lambda^2)} \langle n_2^* n_3^* \rangle - \langle \alpha_{12}^* \rangle^2\end{aligned}$$

where $\langle \alpha_{12}^* \rangle$ is given in Eq. (A22), $\langle n_2^* n_3^* \rangle = \langle n_i^* \rangle^2 = 1/\phi^2$, and $q + \sigma_\lambda^2 = \langle n^2 \rangle + \sigma_K^2 / \sigma^2$.

6. Correlations of interspecies interactions and carrying capacities

The interactions α^* and the vector of carrying capacities of persistent \vec{K}^* become correlated. The derivation of these correlations is very similar to the ones in Sec. A 3, A 5 above, and is only sketched.

Two additional species are introduced, with

$$\begin{aligned}\hat{u}n_1^+ &= \lambda_1 + \eta_1 - a_{12}n_2^+ + h \\ \hat{u}n_2^+ &= \lambda_2 + \eta_2 - a_{21}n_1^+ + h\end{aligned}\quad (\text{A24})$$

where $\eta_i \equiv -\sum_j a_{ij} n_{j \setminus i}$. The joint distribution $P(\lambda_{1,2}, a_{12,21}, n_{1,2}^+)$ is given by

$$JP(a_{12,21})P(\lambda_{1,2})P(\eta_{1,2})$$

where the Jacobian is $J = |\partial \eta_{1,2} / \partial n_{1,2}^+|$. $\eta_{1,2}$ are substituted from Eq. (A24), and $P(\eta_i) = g(\eta_i; \lambda_1 + h, q)$ is expanded to first order in $a_{12,21}$. The conditional distribution is $P(\lambda_{1,2}, a_{12,21} | n_{1,2}^+) = CP(\lambda_{1,2}, a_{12,21}, n_{1,2}^+)$, where the prefactor C depends on $n_{1,2}^+$. The moments of $P(\lambda_{1,2}, a_{12,21} | n_{1,2}^+)$ can now be calculated. As in previous sections, when $n_1, n_2 > 0$, then $n_i^+ = n_i^*$. The new covariance elements read

$$\begin{aligned}\Sigma_{a_{12}, \lambda_1} &= \frac{n_2^*}{S(1 + q/\sigma_\lambda^2)} \\ \Sigma_{a_{12}, \lambda_2} &= \frac{\gamma n_1^*}{S(1 + q/\sigma_\lambda^2)}\end{aligned}$$

Correlations between $\lambda_{1,2}$ and $a_{12,21}$ with no reference to the abundances, are obtained by integrating over $n_{1,2}^*$. The moment $\langle \lambda_1^* a_{12}^* \rangle = \langle \Sigma_{a_{12}, \lambda_1} \rangle + \langle \bar{\lambda}_1 \text{mean}_{n_{1,2}^*} a_{12} \rangle$, where $\bar{\lambda}_1$ is the mean of λ_1 at given n_1^* , see Eq. (A13) and $\text{mean}_{n_{1,2}^*} a_{12}$ is given in Eq. (A20). The covariance $\text{cov}(a_{12}^*, \lambda_1^*)$ reads

$$\langle a_{12}^* \lambda_1^* \rangle - \langle \mu_{12} \rangle \langle \bar{\lambda}_1 \rangle = \frac{\hat{u}(1 + \gamma) \langle n_i^* \rangle - h\gamma}{S(1 + q/\sigma_\lambda^2)} \hat{u} \text{var}(n_i^*)$$

And one may use $\langle n_i^* \rangle = 1/\phi$ and $\langle (n_i^*)^2 \rangle = q/\phi$ to relate these to the model parameters. Similarly, $\text{cov}(a_{12}^*, \lambda_2^*)$ is

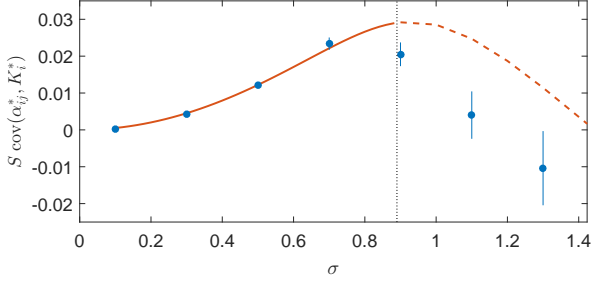


Figure 12. Correlations of carrying capacities and interspecies interactions similar to Fig. 5(c), for $\gamma = 1$ (symmetric α^*), $\mu = 8$ and $\sigma_k = 0.2$.

given by

$$\langle \lambda_2^* a_{12}^* \rangle - \langle \bar{\lambda}_2 \rangle \langle \mu_{12} \rangle = \frac{\sigma_\lambda^2 \langle n_i^* \rangle}{S \sigma_\lambda^2 (1 + q/\sigma_\lambda^2)^2} \begin{bmatrix} (\sigma_\lambda^2 + q) \gamma \langle n_i^* \rangle - \hat{u} h \text{var}(n_i^*) \\ -\gamma \hat{u} h (\langle (n_i^*)^2 \rangle + q \phi \langle n_i^* \rangle^2) \end{bmatrix}.$$

These are translated to $\text{cov}(\alpha_{12}^*, K_1^*)$ and $\text{cov}(\alpha_{12}^*, K_2^*)$ plotted in Fig. 5 by using Eqs. (A2,A4). Fig. 12 shows the covariance for $\gamma = 1$ (here α^* is symmetric so $\text{cov}(\alpha_{12}^*, K_1^*) = \text{cov}(\alpha_{12}^*, K_2^*)$). The analytical results predict that this correlation will be positive. In the second phase, the analytical predictions are approximate, and numerics show a transition to negative correlations.

Appendix B: Phase diagram

Depending on the parameters μ, σ, σ_K and γ , the model exhibits three distinctive phases, which at large S are separated by sharp boundaries, see Figs. 13,14. In the first phase, a given system admits a unique equilibrium solution that is resistant to invasion. In the second phase multiple dynamical attractors generally exist, which may be stable equilibria or other attractors such as limit cycles, and the community composition depends assembly history. In this phase an uninhabitable state might not be reached, and instead invasions trigger jumps between a number of possible communities [11, 20, 22]. This may happen for dynamical attractors [20], or if species that go below some abundance cut-off are removed from the community, as seems inevitable in any realistic situation [11, 20, 22]. In the present model, we only find it in the second phase, and only for asymmetric models (e.g. $\gamma = 0$). This is further discussed in the context of the numerical simulations, Appendix D. The transition between the first and second phase is closely related to those found in various models [13, 16, 27, 30, 40–42], and is also similar to a transition described in [24]. Finally, in the third phase the abundances grow without bound. At smaller values of S the transitions between different regimes is smooth. In particular, for small S the first phase extends further, as smaller systems have a larger probability to have a unique equilibrium.

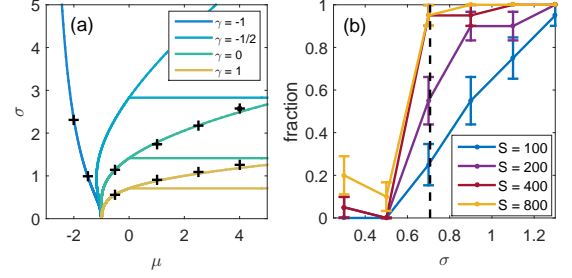


Figure 13. (a) Phase-diagram for $\sigma_K = 0$ and different γ . The $\gamma = 0$ lines correspond to Fig. 2 in the main text. Crosses mark transition to diverging solutions, found numerically. (b) Numerical check of the phase boundary between first and second phases. The fraction of systems (α^*) for which there are multiple solutions, at $\mu = 4$ and $\gamma = 1$. At large S this fraction jumps sharply at the phase-transition. The dashed line marks the analytically calculated transition point, $\sigma = 1/\sqrt{2}$.

The position of the transition to the unbounded growth phase can be calculated by asking where $\langle N \rangle$ diverges. Using the theoretical tools presented in Appendix A, by Eq. (A4), $\langle N \rangle = 1/(\sigma h + \mu)$ so the boundary with the unbounded growth phase lies on the line $\sigma h + \mu = 0$. h is a known function defined in Appendix A, following Eq. (A11). The analytical expression for h is exact in the first phase and approximate in the second, so the prediction for this phase boundary will accordingly be exact when it limits the first phase, and approximate when it limits the second.

The boundary between the first and second phases lies on the line $\phi = (u - \gamma v)^2$, where ϕ is the fraction of persistent species, and v is a known function, see Appendix A. For $\sigma_K^2 = 0$ this line lies at $\sigma = \sqrt{2}/(1 + \gamma)$ for all $\mu > 0$. Along this line the linear response of the abundances to a change in the carrying capacities diverges, indicating loss of stability of the unique equilibrium solution and the appearance of multiple attractors. More precisely, the change of the normalized abundances \vec{n} in response to a perturbation $\vec{\xi}$ defined in Eq. (A5) is $\langle (\delta n)^2 \rangle / \langle \xi^2 \rangle = \phi / [(u - \gamma v)^2 - \phi]$, when the ξ_i 's are sampled independently (the average includes $\delta n_i = 0$ for species outside the community). This transition line can be derived using known techniques [27] similar to the arguments in Appendix A. This phase transition is only encountered when the average interaction is competitive, i.e. for $\mu > 0$ and therefore could not be seen in [26], where a Lotka-Volterra system was studied with $\mu = 0$.

Appendix C: Small S

Figs. 15,16 are identical to Fig. 3(a,b) and Fig. 4, with additional simulations for small pool sizes. As in the main text, the numerical results are plotted as a function of $\sigma = \sqrt{S} \text{std}(\alpha_{ij})$, and the analytical predictions

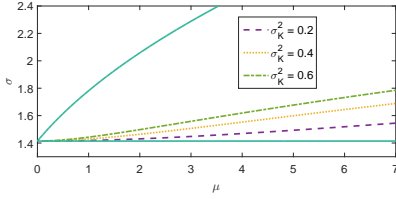


Figure 14. Phase-boundary between first and second phase for different σ_K , at $\gamma = 0$. Solid lines correspond to the $\gamma = 0$ phase boundaries in Fig. 13(a).

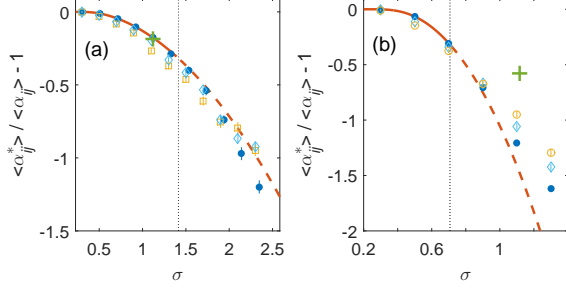


Figure 15. (a,b) are the same as Fig. 3(c,d) respectively, with additional numerical results. Diamonds: α_{ij} sampled from a Gaussian distribution, $S = 25$. Crosses: $S = 15$ with α_{ij} sampled from a uniform distribution on $[0, 1]$.

as a function of $1/u \simeq \sigma$, see Eq. (A4). For normally distributed α_{ij} , numerics for pools of size $S = 15, 25$ are shown in addition to the $S = 200$ results. For $S = 15$, α_{ij} is the mean of is 0.27 and the standard deviation up to 0.6. Another comparison is with α_{ij} sampled from uniform distribution on $[0, 1]$, with $S = 15$ and community sizes of about 6-7 species. The results are in good agreement with numerics even for the $S = 15$ numerics, in the region where the analytics are exact (unique equilibrium phase, left of dotted vertical line).

Depending on the application, one might wish to study models where interactions are purely competitive, or a combination of competitive and beneficial interactions. In addition to the choice of the distribution, the combination of S, μ and σ at a given (e.g., Gaussian) distribution allows for similar control. The fraction of beneficial interactions ($\alpha_{ij} < 0$) is given by the area of the negative tail of $P(\alpha_{ij})$. For $S = 15$ in Figs. 15,16, at $\sigma = 0.5$ only about 2% of the interactions will be beneficial, and only mildly so. Below $\sigma = 0.4$, typically only one or less of the interactions will be beneficial. At larger widths the α_{ij} combine competitive and beneficial interactions.

Appendix D: Numerical simulations

To numerically find persistent solutions, the network variables α_{ij} and K_i are first sampled. α_{ij} are sampled from a normal distribution unless otherwise stated. A

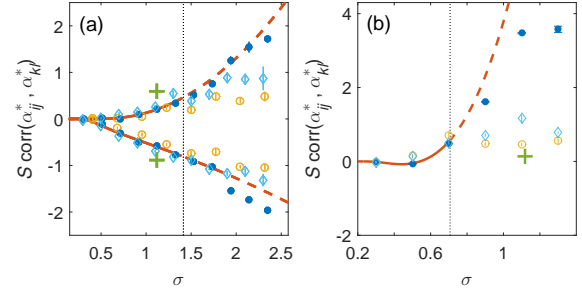


Figure 16. Same as Fig. 3(c,d) respectively, with additional numerical results. Symbols as in Fig. 15.

uniform distribution was checked to give identical results at large S . Results for small S are given in Sec. C.

The Lotka-Volterra dynamics, Eq. (1), are then integrated using a Runge-Kutta 45 solver, from random initial conditions sampled uniformly on $[0, 1]$. All species that go below an abundance cut-off $N_i < 10^{-14}$ are removed from the community (N_i set to zero). The solver is terminated when an equilibrium solution is found, in which for every i either dN_i/dt is small, or $N_i < 10^{-14}$. Solutions that do not terminate are stopped after a long time ($T = 10^7$) and all variables with $N_i > 10^{-14}$ are considered part of the community. The solution is checked against invasion of the pool species not present. As some species are removed during the dynamics due to the abundance cut-off, it is possible that they would be able to invade later. If any such species are found, the dynamics are run from the end point of the first simulation with additional small abundance ($N_i = 10^{-10}$) to the species that may invade. This process is repeated until an uninvadable solution is reached or after ten iterations. In phase one the resulting community is always found to be uninvadable, and usually reached on the first run of the dynamics. For a given system all initial conditions give the same final community. In phase two for asymmetric interactions (specifically $\gamma = 0$), this process did not always converge to an uninvadable solution after ten iterations and then was stopped. All numerical results shown in the paper show only minor differences when plotted after the first run, compared to iterations of the invasion process.

Results large S were simulated with $S = 400$. An exception are the results for $\gamma = 0$ in Figs. 3,4 which were run with $S = 200$. This was chosen as balance finite-size effects while minimizing the number of species that can invade in phase two: The results for $S = 100$ and $S = 200$ are very similar, indicating good finite-size convergence, and both have a small fraction (less than 0.05, see Fig. 17). Other options are possible, and would represent ecological conditions with varying effects of the minimal allowed abundance.

To test for multiplicity of equilibria, as shown in Fig. 13(b), the same system (same α_{ij} and K_i) is run starting from different initial conditions.

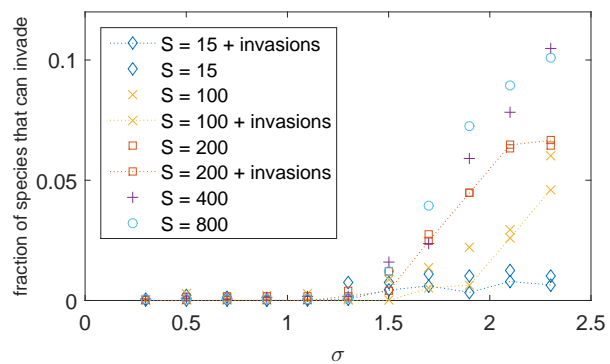


Figure 17. Fraction of species that may invade. Data plotted with dashed lines show the results after multiple invasion attempts.